International Journal of Technology 13(2) 332-344 (2022)
Received May 2021 / Revised May 2021 / Accepted June 2021

International Journal of Technology

http://ijtech.eng.ui.ac.id

Experimental Investigation of Added Resistance of a Ship using a Hydroelastic Body in Waves

Suandar Baso[1*], Andi Ardianti[1], Andi Dian Eka Anggriani[1], Rosmani[1], Lukman Bochary[1]

[1]*Naval Architecture Department, Faculty of Engineering, Hasanuddin University, Jl. Perintis Kemerdekaan Km.10, 90245, Makassar, Indonesia*

Abstract. Ship resistance is an important characteristic to predict in the preliminary design stage. Proper prediction of ship resistance implies the fulfillment of the required speed and power of a ship. The assumed body characteristics of a ship model should also be properly considered when investigating ship resistance. In the present study, the assumption of a hydroelastic body for a ship model was used in an experiment on total ship resistance and added resistance in calm water and waves. Two hydroelastic models were used: a hydroelastic body with a bulbous bow (HB) and a hydroelastic body without a bulbous bow (HWB). The wavelength considered ranged from 0.5 L to 1.3 L, and the Froude number (Fn) considered ranged from 0.058 to 0.232. In the presented results, the total resistance coefficient of the HWB was higher than that of a rigid body without a bulbous bow (RWB). The average difference of magnitude between the HWB and RWB was 30.49% for calm water conditions and 30.37% for overall wave conditions. The total resistance of the HB was higher than that of the rigid body with a bulbous bow (RB), and the difference of magnitude was approximately 31.47% for calm water conditions and 31.68% for overall wave conditions. The added resistance coefficient of the HWB tended to increase with an increase in the wavelength, from 0.5 L to 1.1 L, and then decrease until 1.5 L. The overall tendency of the added resistance coefficient of the HB was significantly different from the other numerical results. Although the tendencies were different, most of the presented results were in the same range as the other numerical results.

Keywords: Added resistance; Hydroelastic body; Rigid body; Ship resistance experiment; Total resistance

1. Introduction

A ship in waves experiences certain phenomena due to extreme ship–wave interactions, and this condition can lead to dangerous risks. Although a ship has an internal ability to counter some external disturbances, regardless of its performance, there are limitations. For this reason, the performance of a ship can be improved in many ways through the body form design, structural design, additional appendages, etc. Therefore, a proper ship design is very desirable and should be focused foremost on ship hydrodynamic considerations.

The proper prediction of the resistance of a ship design has implications for the ship's operational cost. Therefore, added resistance due to waves must be predicted

*Corresponding author's email: s.baso@eng.unhas.ac.id, Tel.: +62-411-589707, Fax: +62-411-589707
doi: 10.14716/ijtech.v13i2.4904

simultaneously with resistance in calm water.

In the past decade, there have been several investigations of the added resistance of a ship in waves, both short and long waves (Duan & Li, 2013; Ageno et al., 2015; Chen & Duan, 2015; el Moctar et al., 2015; Liu et al., 2015; Park et al., 2016; Sigmund & el Moctar, 2018; Park et al., 2019a), regular incident waves (Cepowski, 2016; Ozdemir & Barlas, 2017; Kim et al., 2017(c); Kim et al., 2017a; Kim et al., 2017b; Lee et al., 2019; Cepowski, 2020), irregular waves (Cepowski, 2020), in the presence of wind–wave loads (Kim et al., 2017b; Wang et al., 2019), and oblique waves (Kim et al., 2017b; Islam et al., 2019; Park et al., 2019a).

Besides the consideration of the influence of waves and wave-induced motions on added resistance, the influences of internal aspects of the ship have been taken into account as well, focusing on large blunt ship designs (Duan & Li, 2013; Chen & Duan, 2015), speed (Duan & Li, 2013; Cepowski, 2016; Ozdemir & Barlas, 2017; Kim et al., 2017c; Kim et al., 2017a; Kim et al., 2017b; Cepowski, 2020), ship type (el Moctar et al., 2015; Cepowski, 2016; Park et al., 2016; Sigmund & el Moctar, 2018; Islam et al., 2019; Lee et al., 2019; Park et al., 2019a; Wang et al., 2019), sectional form (Liu et al., 2015), and geometrical parameters (Cepowski, 2016; Cepowski, 2020).

Some methods that have been used to predict added resistance have been widely discussed, including the radiated energy theory along with the strip method (Duan & Li, 2013; Park et al., 2016; Park et al., 2019a), second-order Taylor Expansion Boundary Element Method/TEBEM (Chen & Duan, 2015), RANS (el Moctar et al., 2015; Sigmund & el Moctar, 2018; Islam et al., 2019), analytical and semi-empirical formulas (Liu et al., 2015), the Rankine panel method (Ageno et al., 2015; Park et al., 2016; Park et al., 2019a), finite volume CFD code (Ozdemir & Barlas, 2017), artificial neural networks (Cepowski, 2016; Cepowski, 2020), URANS (Kim et al., 2017c; Lee et al., 2019; Wang et al., 2019), URANS CFD and 3D potential methods (Kim et al., 2017a; Kim et al., 2017b). The use of these methods has yielded accurate results and, when compared with experimental results, they seem to be in good agreement.

The assumption of a rigid body in the prediction of resistance and added wave resistance has been widely used. However, the influence of a hydroelastic body in these predictions has not been considered, even though it is real. Meanwhile, other investigations of ship–wave interactions, including induced motions, slamming impact, and whipping impact, consider the assumption of a hydroelastic body, and this assumption has been adopted widely. In general, a rigid body, due to ship–wave interaction, experiences small deformation, but the interaction is affected not only by the body's deformation but also by water deformation. Therefore, water deformation due to ship–wave interaction inevitably influences the ship's added resistance. To consider water deformation, hydrodynamic analysis of ships in the investigation of added resistance should be considered in both numerical methods and experimental work. However, so far, the added resistance of a hydroelastic body or a flexible body has been investigated only rarely. A segmented barge was considered in a hydroelastic analysis wherein additional resistance due to pontoon motion was induced by the relative angular velocity (Senjanovic et al., 2017), but this was discussed only briefly. In another study, the added resistance of a flexible ship was investigated numerically, and the deformation and added resistance obtained were small (Park et al., 2019b), but the added resistance was not validated with experimental data.

As an encapsulation of the above statements, the prediction of the wave-induced resistance of a ship remains challenging. With the objective of a systematic investigation of ship resistance and added resistance, the assumption of a hydroelastic body should be considered to enhance the ship's body characteristics as well as to obtain some

interpretation of the influence of a hydroelastic body on resistance and added resistance in waves, after which the hydrodynamic interpretation can be considered to produce a proper ship design in the preliminary design stage. Therefore, in the present study, the resistance and added resistance of a ship were investigated experimentally. For the experimental investigation, the ship model was divided into several segmented bodies considered as a hydroelastic body. Also, the resistance and added resistance of a rigid model were investigated experimentally for comparison with the resistance and added resistance of the hydroelastic body.

2. Methods

In the present study, the investigation of ship resistance in calm water and waves was carried out using an experimental method and ship models of both a hydroelastic body and a rigid body. Also, the effect of a bulbous bow was investigated. In the following, the ship model and the experimental set-up are discussed.

2.1. Ship Model

The investigated ship type was general cargo, with the main dimensions of the ship and its body lines plan shown in Table 1 and Figure 1, respectively.

Table 1 The Main Details of an Actual Ship and the Ship Model

Dimension	Actual Ship	Model
Length overall/Loa (m)	73.30	1.83
Length waterline/Lwl (m)	72.10	1.80
Length between perpendiculars/Lbp (m)	70.10	1.75
Breadth/B (m)	11.50	0.29
Depth/H (m)	7.00	0.18
Draft/T (m)	5.50	0.14

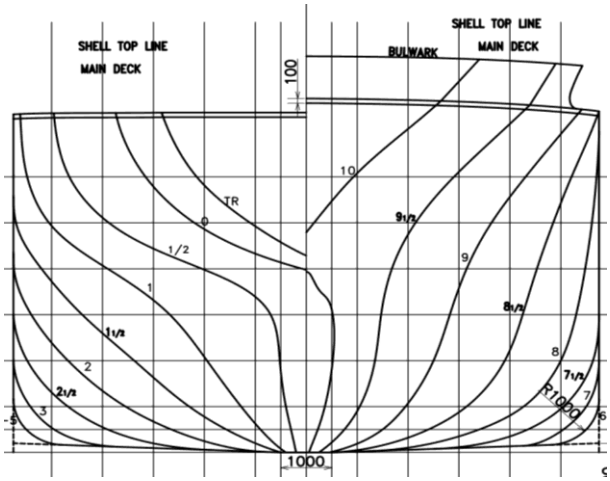

Figure 1 The body lines plan

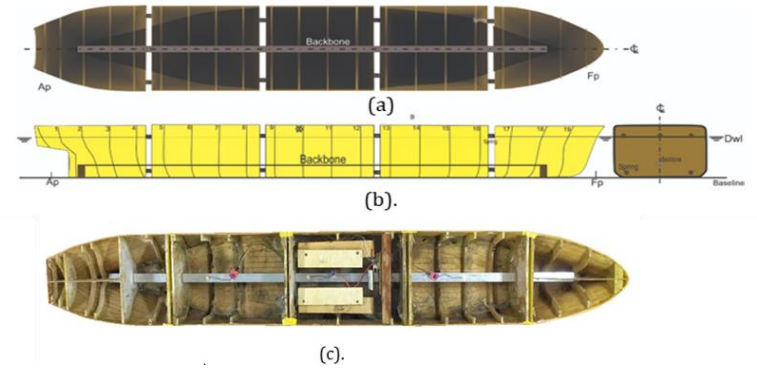

Figure 2 Model of the hydroelastic body: (a) sketch of the segmented model, top view; (b) sketch of the hydroelastic body, side view; and (c) physical model of the hydroelastic body.

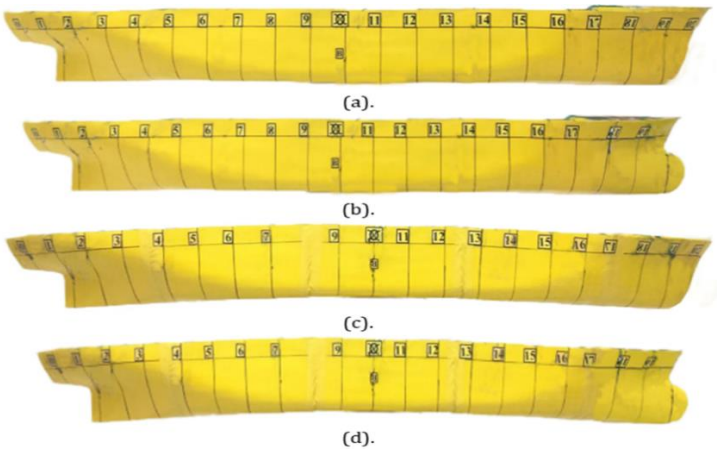

Figure 3 The four models employed in the experiment: (a) model RWB; (b) model RB; (c) model HWB; and (d) model HB.

2.2. Experimental Set-up

The experimental work was conducted at the towing tank of the Ship Hydrodynamics Laboratory, Department of Naval Architecture, Hasanuddin University. The towing tank dimensions were 60 m in length, 4 m in width, 6 m in depth, and 3.80 m in water depth. The speed of the towing carriage was a maximum of 4 m/sec, and the towing tank was equipped with a wavemaker.

In the experiment, the wave was propagated as a regular heading wave with various wavelengths of 0.29 m (0.5 Lwl), 1.46 m (0.8 Lwl), 1.83 m (1.0 Lwl), 2.01 m (1.1 Lwl), and 2.38 m (1.3 Lwl), and the wave amplitude was given as 0.004 m based on the setting of the wave frequency, which was 1.31 Hz, 1.01 Hz, 0.92 Hz, 0.88 Hz, and 0.81 Hz to refer to the wavelengths, respectively. As an example, the time history of waves within a propagation time of 120 sec based on the wave frequency is shown in Figure 4. The ratio of the wave height to the depth-draft was 0.2. For Froude similarity, the wave pattern produced by the geometrical similarity of the model and the ship was the same when the model and the ship traveled at the same speed as the square root of the length ratio, or V_M, obtained by $V_s*\sqrt{L_M}/\sqrt{L_s}$, or Fn, obtained by $V_M/\sqrt{gL_M}$. Several model speeds were considered, namely 0.244 m/sec (Fn = 0.058), 0.488 m/sec (Fn = 0.166), 0.732 m/sec (Fn = 0.174), and 0.976 m/sec (Fn = 0.232). The experimental scheme is illustrated in Figure 5.

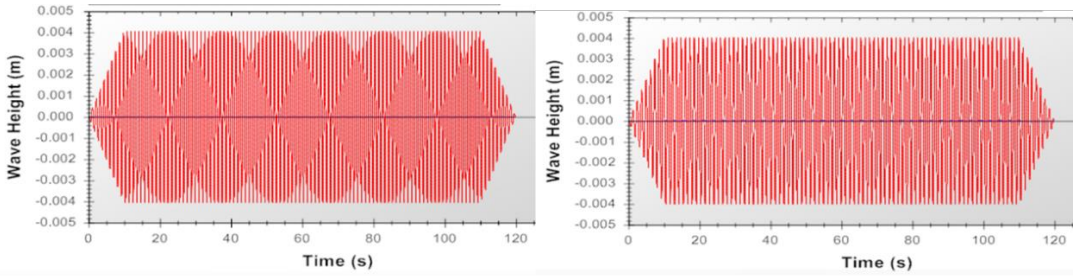

(a) (b)

Figure 4 Time history of a wave within 120 sec: (a) wave frequency of 0.92 Hz and a length of 1.83 m; and (b) wave frequency of 0.81 Hz and a length 2.38 m

The hydroelastic model used was a flexible model divided into five segmented bodies as illustrated in Figure 2a. Each segmented body was connected using a spring and a thin plate as a backbone, as shown in Figure 2b. One side or two sides of the segmented model were closed and watertight. The gap between each segmented body was close to 0.005 m, and it was covered tightly with a strong, flexible, and very sticky tape. Four models were employed in the experiment, as shown in Figure 3, namely a rigid model without a bulbous bow (RWB), a rigid model with a bulbous bow (RB), a hydroelastic body without a bulbous bow (HWB), and a hydroelastic body with a bulbous bow (HB).

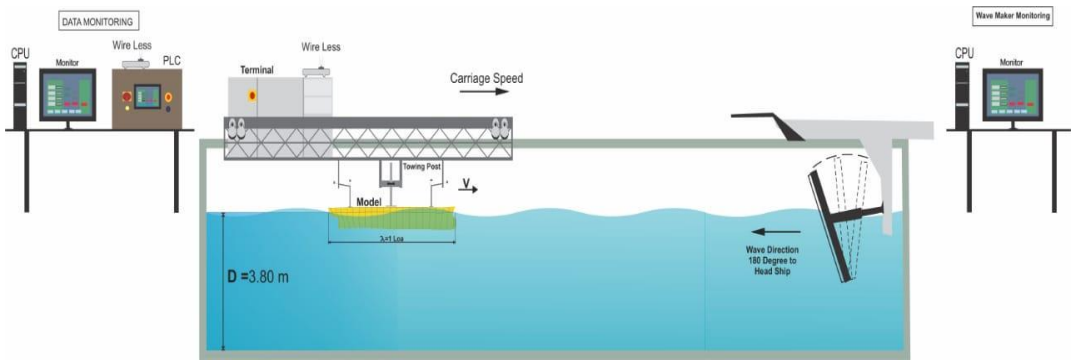

Figure 5 Experimental scheme of the ship resistance test in waves

3. Results and Discussion

The total resistance of the RWB and the RB in calm water ($R_{calm\ water}$) and waves (R_{wave}) was obtained during the experimental work, the data of which are discussed here using the term of the total resistance coefficient (C_t), Equation (1) and Equation (2), which is defined as follows:

$$C_t = \frac{R_{Calm\ water}}{0.5\rho S V^2} \quad (1)$$

and

$$C_t = \frac{R_{wave}}{\rho g \zeta^2 B^2 / L} \quad (2)$$

$R_{calm\ water}$ is the total resistance in calm water, R_{wave} is the total resistance in waves, ρ is the water density, S is the wetted area, V is the ship speed, ζ is the wave amplitude, g is the gravitational acceleration, B is the breadth of the ship, and L is the length of the water line. The total resistance in waves is proportional to the wave height squared. Therefore, the total resistance coefficient in waves is further described against the speed or Fn.

During the measurement, uncertainties were detected in some of the data on total resistance, a problem that was prevented by repeating the measurement and checking to

ensure that the mean error was less than 5.0%. Accordingly, the investigation of the total resistance and added resistance in waves due to the rigid body and hydroelastic body is discussed systematically below.

3.1. Resistance of the Rigid Body in Calm Water and Waves

The tendency of the coefficient of total resistance in calm water was to decrease with increasing speed or Fn, as shown in Figure 6(a)—nevertheless, the tendency of the coefficient of total resistance in waves was to increase with increasing speed or Fn, as shown in Figure 6(b, c, d, e, and f), but the total resistance was different for each water condition. The discrepancy of the coefficient of total resistance between the RWB and the RB with increasing Fn seemed to be relatively of the same magnitude, as shown in Figure 6, and a small difference in calm water occurred at Fn 0.232; otherwise, a small difference in waves occurred at 0.174.

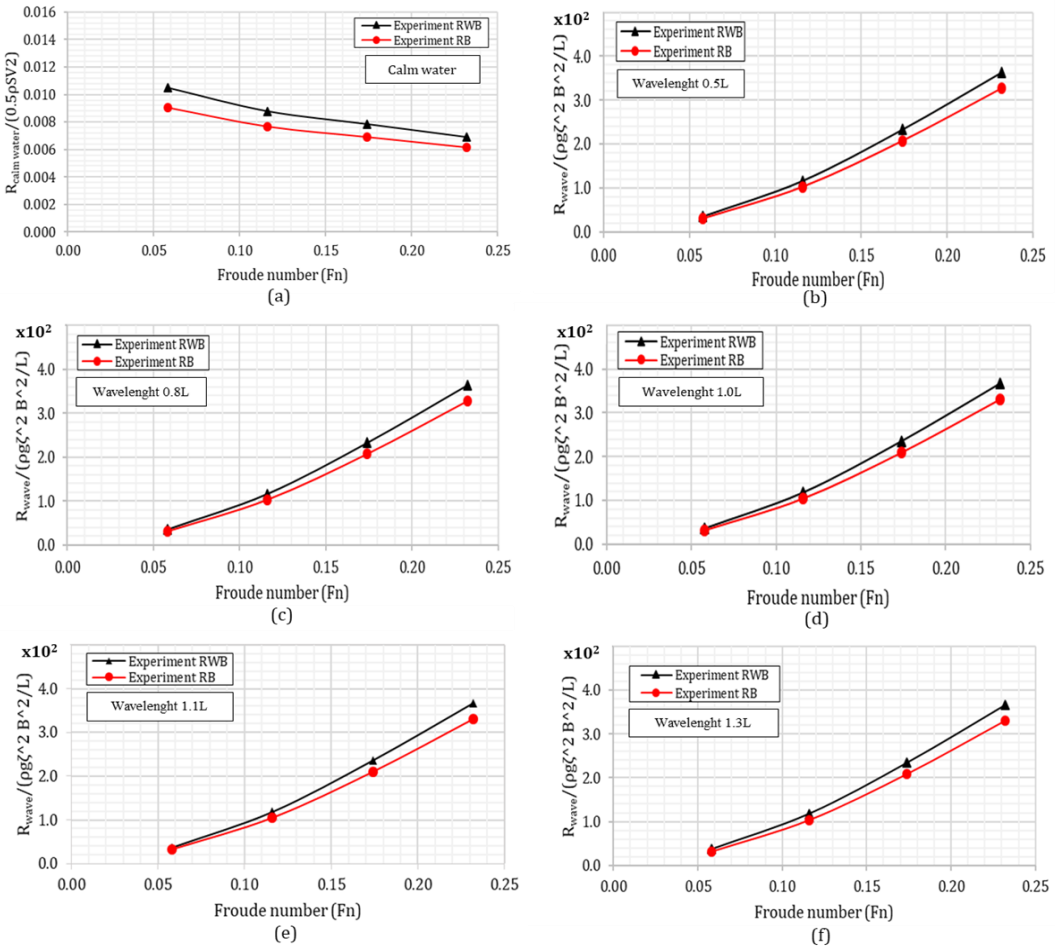

Figure 6 Tendency of the coefficient of total resistance of the RWB and the RB with increasing Fn in the water conditions: (a) calm water; (b) wavelength 0.5 L; (c) wavelength 0.8 L; (d) wavelength 1.0 L; (e) wavelength 1.1 L (f) wavelength 1.3 L

Meanwhile, the influence of the bulbous bow was indicated by the reduction of the total resistance, including in waves, as shown in the results of the comparison between the RWB and the RB. Based on the discrepancy of the coefficient of total resistance between the RWB and the RB, due to the effect of the HB, the total resistance was reduced by an average of 11.08% in calm water, 11.22% in 0.5 L, 11.36% in 0.8 L, 11.71% in 1.0 L, 11.12% in 1.1 L, and 11.47% in 1.3 L. In short waves, the discrepancy between the RB and the RWB was higher than in long waves. Based on these results, the total resistance was reduced by an

average of 11.47%. As observed consecutively during the experiment, the RWB generated a cresting wave in the bow region, whereas the RB generated a trough wave in the bow region, in addition to which the longitudinal and transverse waves also seemed different when comparing the RWB and RB models. With increasing Fn, the tendency of longitudinal and transverse waves seemed to be large.

Furthermore, in almost all cases for both the RWB and the RB, the total resistance increased when increasing the wavelength at a constant speed, but decreased at 0.8 L and 1.3 L. This result clarifies other research findings that the prediction of ship resistance must take into account wave conditions in the ship design stage. In this investigation, the total resistance due to waves increased by approximately 11.35%.

The coefficient of total resistance at 1.1 L with an increase of the Fn for both the RWB and the RB was higher than in the other wavelength conditions. Also, the coefficient of total resistance due to shifting the water condition from calm water to wavelengths for all Fn values increased until it reached 1.1 L, after which it decreased until reaching the wavelength of 1.3 L. This means that the peak of the coefficient of total resistance was at a wavelength of 1.1 L.

3.2. Resistance of the Hydroelastic Body in Calm Water and Waves

Referring to Equations (1) and (2), Figure 7 shows the tendency of the coefficient of total resistance for both the HWB and the HB to decrease with an increasing Fn in calm water and to increase with an increasing Fn in waves. However, the coefficient of total resistance in waves at Fn 0.174 increased after reaching Fn 0.116, and the same tendency was seen for all cases of the wave condition. The total resistance at Fn 0.232 was higher than at the other Fn values. From the comparison between the HWB and the HB, the coefficient of total resistance seemed to be significantly different with the increase of the Fn, wherein the coefficient of total resistance of the HWB was higher than that of the HB, with an average of 9.72% for the wavelength 1.3 L. Eventually, the overall discrepancy was an average of 9.81%, and from this obtained result, the effect of the HB in terms of the use of the hydroelastic body also had an impact on the reduction of the resistance.

The increase of the coefficient of total resistance with the increasing wavelength with a constant Fn was relatively small, wherein the discrepancy between the HWB and the HB at constant Fn was an average of 9.81%. In addition, the increase in the coefficient of total resistance for the HWB at a constant Fn was an average of 0.48%, whereas it was an average of 0.62% for the HB. These findings indicate that the total resistance increases on a relatively small scale with the increasing wavelength at a constant speed. Nevertheless, the indication of the effect of the hydroelastic body in waves should be identified later in relation to the added resistance.

Based on the above discussion, the investigation of the total resistance in the case of the use of the rigid body and the hydroelastic body demonstrated a significant difference. The coefficient of total resistance of the HWB was higher than that of the RWB. The difference of magnitude between the HWB and the RWB was an average of 30.49% for calm water and 30.37% for the overall wave condition. For the case of the RB and the HB with bulbous bows, the total resistance tended to increase with an increasing Fn, and the highest total resistance was obtained in the wavelength 1.1 L. From the comparison, the coefficient of total resistance of the HB was higher than that of the RB, and this difference was approximately 31.47% for calm water and 31.68% for the wave condition. From the above findings, by using the hydroelastic body in the prediction of ship resistance, the total resistance in calm water and waves can be considered to be increased.

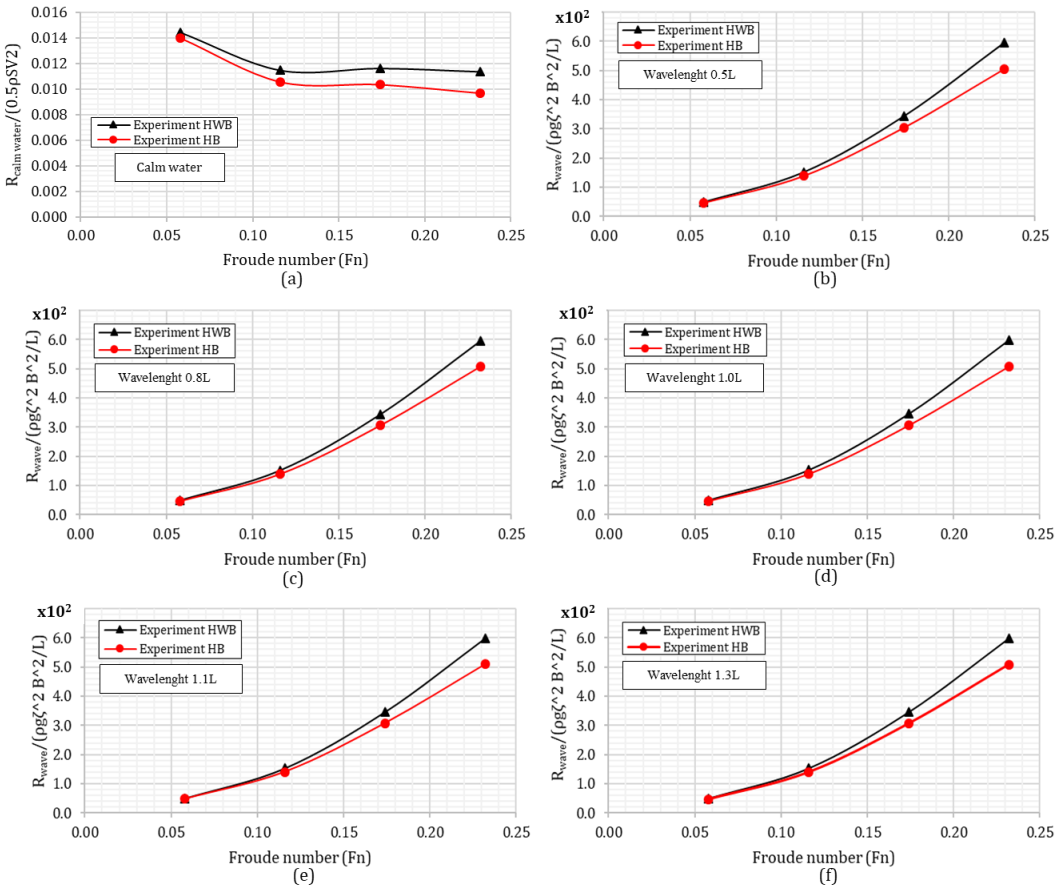

Figure 7 Tendency of the coefficient of total resistance of the HWB and the HB with an increasing Fn in water conditions: (a) calm water; (b) wavelength 0.5 L; (c) wavelength 0.8 L; (d) wavelength 1.0 L; (e) wavelength 1.1 L (f) wavelength 1.3 L.

3.3. Added Resistance of the Rigid and Hydroelastic Bodies

Here, the added resistance was discussed accordingly. The ship resistance in waves stated in the previous sections consists of two components, which are the resistance in calm water and the added resistance. The added resistance can be obtained by subtracting the resistance in calm water from the resistance in waves as given in Equation (3). Then, the added resistance coefficient is normalized and defined in Equation (4) as follows:

$$R_{aw} = R_{wave} - R_{calm\ water} \tag{3}$$

$$C_{aw} = \frac{R_{aw}}{\rho g \zeta^2 B^2 / L} \tag{4}$$

R_{aw} is the added wave resistance, R_{wave} is the total resistance in waves, $R_{calm\ water}$ is the total resistance in calm water, C_{aw} is the added resistance coefficient, ρ is the water density, ζ is the wave amplitude, g is the gravitational acceleration, B is the breadth of the ship, and L is the length of the water line. As with the coefficient of total resistance, the coefficient of the added resistance is proportional to the wave height squared. Then, the added resistance coefficient is described against the ratio of wavelength to ship model length and increasing speed or Fn.

Many studies of added resistance have been carried out experimentally by several researchers (Kashiwagi, 2013; Valanto & Hong, 2015; Park et al., 2019a). In the experiments, several ship models were employed—namely, the blunt modified Wigley model (Kashiwagi, 2013), the two models used at the SNU towing tank (model with an extended vertical shape above the deck line) and the SSPA basin (Park et al., 2019a), and the model of 1001 (bow shape with a bulbous bow) and 2101 (bow shape without a bulbous

bow/vertical bow) (Valanto & Hong, 2015). The ship model used had a rigid body. From the investigation results, the tendency of the coefficient of added resistance in short waves increased when the wavelength was less than the length of the ship. The peak coefficient of the added resistance was obtained in the range of the wavelength to ship length ratios of 1.0 to 1.3, as shown in Figure 8 and 9.

Concerning the present study, the added resistance coefficient from 0.5 L to 1.0 L showed the same tendency as the other results (Kashiwagi, 2013; Valanto & Hong, 2015; Park et al., 2019a). The distribution of the added resistance coefficient was nearly in the range shown in Figure 8 and 9. Therefore, in the present results, the added resistance of the RWB and the RB agreed well with the other results. Meanwhile, as of yet, no other experimental investigation of added resistance using the hydroelastic body has been conducted. In a numerical investigation only, Park et al. (2019b) investigated the added resistance of a flexible ship (the blunt modified Wigley model), so their research results were used for comparison with the present results (experimental results).

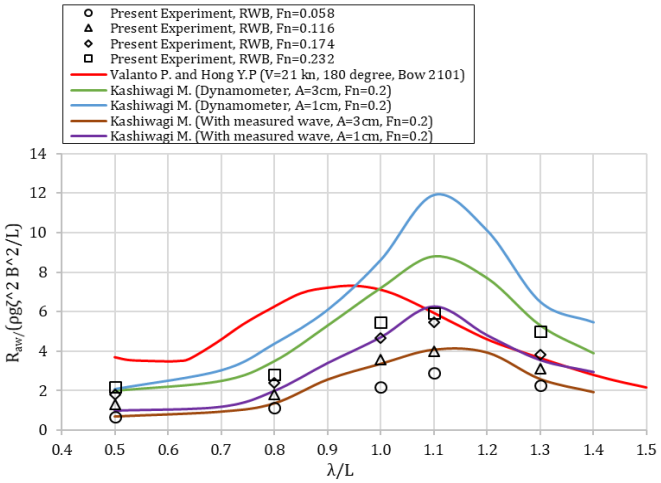

Figure 8 Tendency of the added resistance coefficient of the RWB compared with other results

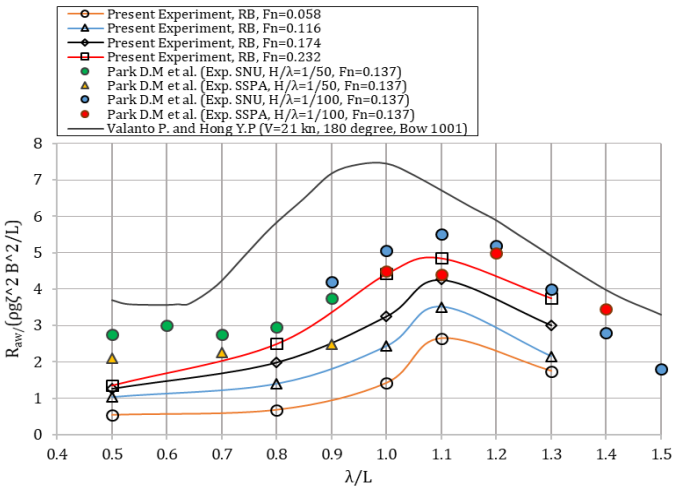

Figure 9 Tendency of the added resistance coefficient of the RB compared with other results

Figure 10 and 11 show the added resistance coefficient of the HWB and the HB in the wavelength range of 0.5 L to 1.5 L, respectively. Based on Figure 10, the tendency of the added resistance coefficient of HWB increased as the wavelength increased from 0.5 L to 1.1 L, and then decreased until 1.5 L. The peak of the added resistance coefficient of the hydroelastic body occurred at 1.1 L, and this confirms a good agreement with the rigid body,

as seen in other results (Kashiwagi, 2013; Valanto & Hong, 2015; Park et al., 2019a). Also, the overall HWB cases showed the same tendency as the RWB. For the case of the HWB, the present results were compared with the other results (Park et al., 2019b), as shown in Figure 10. The overall tendency of the added resistance coefficient was significantly different from these other results (Park et al., 2019b). All of the added resistance coefficients in the present results had a peak tendency at 1.1 L, whereas they were in the range of 0.7 L to 0.9 L in the findings of Park et al. (2019b). Although the tendencies were clearly different, almost all of the added resistance coefficients in the short wavelength from 0.5 L to 0.9 L were lower than in the range of the other results (Park et al., 2019b). In long wavelengths, from 1.1 L to 1.3 L, almost all of the added resistance coefficients in the present results were obviously larger than those in the other results (Park et al., 2019b).

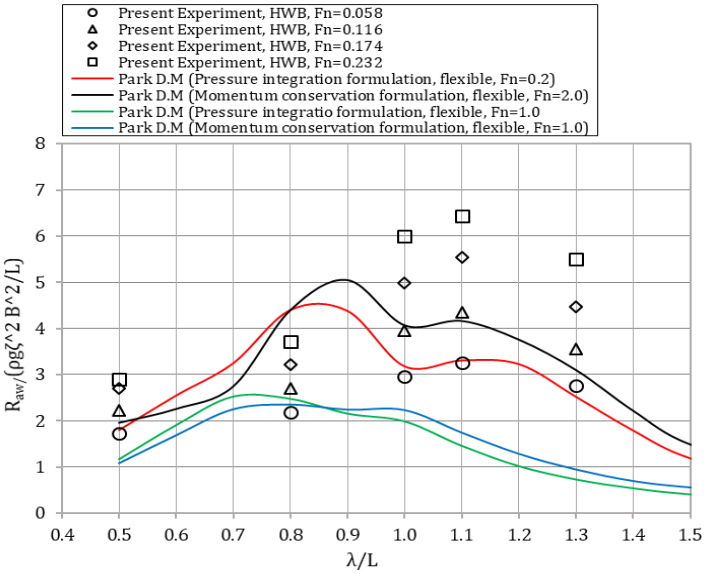

Figure 10 Tendency of the added resistance coefficient of the HWB (experimental results) compared with other numerical results.

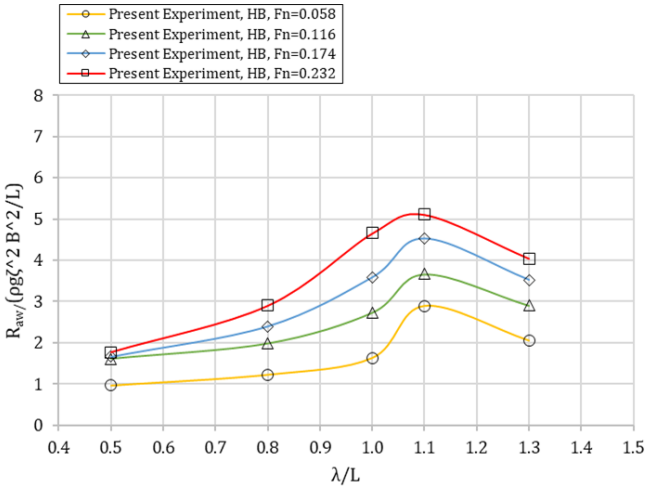

Figure 11 Tendency of the added resistance coefficient of the HB (experimental results).

For the case of the hydroelastic body with a bulbous bow (HB), no other experimental or numerical investigations of added resistance using the hydroelastic body have yet been conducted. Figure 11 shows the tendency of the added resistance coefficient, wherein it increased as the wavelength increased, from 0.5 L to 1.1 L, and then decreased until 1.5 L. The peak of the added resistance coefficient of the hydroelastic body occurred at 1.1 L,

which confirms a good agreement with the rigid body, as seen in other results (Kashiwagi, 2013; Valanto & Hong, 2015; Park et al., 2019a). Also, the overall HB cases showed the same tendency as the RB. For comparison with the HWB, the tendency of the added resistance coefficient was similar but the added resistance coefficient of the HB was lower than that of the HWB.

In the experiment, the wave profile due to ship motions (heave and pitch), speeds, and waves showed a different magnitude between short and long waves, and this was reflected in the results of the added resistance. In certain long waves, the ship motions become large when both the hydroelastic body with and without a bulbous bow have higher heave and pitch amplitudes at a wavelength of 1.1 L; therefore, the peak of the added resistance coefficient of them both appears at 1.1 L.

Based on the overall discussion above, in this present result, the behaviour of the hydroelastic body in the investigation of ship resistance is the same as that of the rigid body, and this behaviour implies the same for the investigation of the added resistance. As stated previously, the tendency of the added resistance coefficient of the hydroelastic body is the same as that of the rigid body, but the coefficient of added resistance is different, being greater for the hydroelastic body than for the rigid body.

Regarding the various hull forms of the planing hull, several experimental investigations of the total resistance using rigid body in calm water were conducted such as the floating catamaran pontoon for N219 seaplanes based on biomimetics design with clearance configuration [Yanuar et al., 2018], the effects of the application of a stern foil [Suastika et al., 2018], the axe-bow applied to a trimaran for total resistance reduction [Utama et al., 2021], etc. Therefore, an experimental investigation of the total resistance and added resistance of a small ship or semi planing hull using hdyroelastic body will be a concern point and considered to carry out in the future work.

4. Conclusions

Resistance tests of a model ship using a rigid body and a hydroelastic body in calm water and waves were performed successfully. The investigation of the total resistance and the added resistance due to the hydroelastic body was discussed, and the influence of the hydroelastic body on the magnitude of the resistance and added resistance was investigated. In this present study, the notable contributions were presented accordingly. The total resistance in calm water and waves, for the hydroelastic body, significantly increased with both increasing Fn and increasing wavelength at a constant Fn. The tendency of the total resistance using the hydroelastic body was similar to that of the rigid body. Using the hydroelastic body without a bulbous bow, the increase of total resistance in calm water and waves was an average of 30.49% and 30.37%, respectively. Meanwhile, using the hydroelastic body with a bulbous bow, the increase of the total resistance in calm water and waves was an average of 31.47% and 31.68%, respectively. The added resistance coefficient of the hydroelastic body with and without a bulbous bow tended to increase with an increase of the wavelength, from 0.5 L to 1.1 L, and then decrease until 1.5 L. The peak of the added resistance coefficient of both the hydroelastic body with and without a bulbous bow occurred at 1.1 L. The overall results showed the same tendencies as the rigid body as well as confirming a good agreement with other numerical results. The effect of the hydroelastic body on ship resistance was the same as that for the rigid body, and this behavior was also the same in the added resistance investigation.

References

Ageno, E., Begovic, E., Bruzzone, D., Galli, A.M., Gualeni, P., 2015. A Boundary Element Method for Motions and Added Resistance of Ships in Waves. *Transactions of Famena*, 39(2), pp. 1–12

Cepowski, T., 2016. Approximating the Added Resistance Coefficient for a Bulk Carrier Sailing in Head Sea Conditions Based on Its Geometrical Parameters and Speed. *Polish Maritime Research*, Volume 23(4), pp. 8–15

Chen, J., Duan, W., 2015. Added Resistance Simulation of Blunt Ship in Short Wave. *In:* Proceedings of the 30th International Workshop on Water Waves and Floating Bodies, Bristol, United Kingdom, pp. 12–15

Cepowski, T., 2020. The Prediction of Ship Added Resistance at the Preliminary Design Stage by the Use of an Artificial Neural Network*. Ocean Engineering*, Volume 195, pp. 1–14

Duan, W., Li, C., 2013. Estimation of Added Resistance for Large Blunt Ship in Waves. *Journal of Marine Science and Application,* Volume 12, pp. 1–12

el Moctar, O., Sigmund, S., Schellin, T.E., 2015. Numerical and Experimental Analysis of Added Resistance of Ships in Waves. *In:* Proceedings of the 34th International Conference on Ocean, Offshore and Arctic Engineering, St. John's, Newfoundland, Canada, May 31–June 5

Islam, H., Rahaman, M.M., Akimoto, H., 2019. Added Resistance Prediction of KVLCC2 in Oblique Waves. *American Journal of Fluid Dynamics*, Volume 9(1), pp. 13–26

Kashiwagi, M., 2013. Hydrodynamic Study on Added Resistance Using Unsteady Wave Analysis. *Journal of Ship Research*, Volume 57(4), pp. 220–240

Kim, M., Hizir, O., Turan, O., Incecik, A., 2017a. Numerical Studies on Added Resistance and Motions of KVLCC2 in Head Seas for Various Ship Speeds. *Ocean Engineering*, Volume 140, pp. 466–276

Kim, M., Hizir, O., Turan, O., Day, S., Incecik, A., 2017b. Estimation of Added Resistance and Ship Speed Loss in Seaway. *Ocean Engineering*, Volume 141, pp. 465–476

Kim, Y.C., Kim, K.S., Kim, J., Kim, Y., Park, R., Jang, Y.H., 2017c. Analysis of Added Resistance and Seakeeping Responses in Head Sea Conditions for Low-Speed Full Ships Using URANS Approach. *International Journal of Naval Architecture and Ocean Engineering*, Volume 9(6), pp. 641–654

Lee, C.M., Park, S.C., Yu, J.W., Choi, J.E., Lee, I., 2019. Effects of Diffraction in Regular Head Waves on Added Resistance and Wake Using CFD. *International Journal of Naval Architecture and Ocean Engineering*, Volume 11(2), pp. 736–749

Liu, S., Papanikolaou, A., Zaraphonitis, G., 2015. Practical Approach to the Added Resistance of a Ship in Short Waves. *In:* Proceedings of the 25th International Ocean and Polar Engineering Conference, Kona, Big Island, Hawaii, USA, 21–26 June, pp. 11-18

Ozdemir, Y.H., Barlas, B., 2017. Numerical Study of Ship Motions and Added Resistance in Regular Incident Waves of KVLCC2 Model. *International Journal of Naval Architecture and Ocean Engineering*, Volume 9(2), pp. 1–11

Park, D.M., Kim, Y., Seo, M.G., Lee, J., 2016. Study on Added Resistance of a Tanker in Head Waves at Different Drafts. *Ocean Engineering*, Volume 111, pp. 569–581

Park, D.M., Lee, J.H., Jung, Y.W., Lee, J., Kim, Y., Gerhardt, F., 2019a. Experimental and Numerical Studies on Added Resistance of Ship in Oblique Sea Conditions. *Ocean Engineering*, Volume 186, pp. 1–14

Park, D.M., Kim, J.H., Kim, Y., 2019b. Numerical Study of Added Resistance of Flexible Ship. *Journal of Fluids Structures*, Volume 85(3), pp. 199–219

Senjanovic, I., Malenica, S., Tomasevic, S., Rudan, S., 2017. Methodology of Ship Hydroelasticity Investigation. *Brodogradnja*, Volume 58(2), pp. 133–145

Sigmund, S., el Moctar, O., 2018. Numerical and Experimental Investigation of Added Resistance of Different Ship Types in Short and Long Waves. *Ocean Engineering*, Volume 147, pp. 51–67

Suastika, K., Hidayat, A., Riyadi, S., 2017. Effects of the Application of a Stern Foil on Ship Resistance: A Case Study of an Orela Crew Boat. *International Journal of Technology*, Volume 8(7), pp. 1266–1275

Utama, I.K.A.P., Sutiyo, Suastika, K., 2021. Experimental and Numerical Investigation into the Effect of the Axe-Bow on the Drag Reduction of a Trimaran Configuration. *International Journal of Technology,* Volume 12(3), pp. 527–538

Valanto, P., Hong, Y.P., 2015. Experimental Investigation on Ship Wave Added Resistance in Regular Head, Oblique, Beam, and Following Waves. *In:* Proceedings of the 25th International Ocean and Polar Engineering Conference, Kona, Big Island, Hawaii, USA, 21–26 June, pp. 19–26

Wang, W., Wu, T., Zhao, D., Guo, C., Luo, W., Pang, Y., 2019. Experimental–Numerical Analysis of Added Resistance to Container Ships Under Presence of Wind–Wave Loads. *PloS ONE*, Volume 14, pp. 1–29

Yanuar, Gunawan, Utomo, A.S.A., Luthfi, M.N., Baezal, M.A.B., Majid, F.R.S., Chairunisa, Z., 2020. Numerical and Experimental Analysis of Total Hull Resistance on Floating Catamaran Pontoon for N219 Seaplanes based on Biomimetics Design with Clearance Configuration. *International Journal of Technology*, Volume 11(7), pp. 1397–1405